



# Multi-platform remote sensing of new production in central California during the 1997–1998 El Niño

R.M. Kudela <sup>a,\*</sup>, F.P. Chavez <sup>b</sup>

<sup>a</sup> Ocean Sciences Department, University of California, Santa Cruz , 1156 High Street, Santa Cruz, CA 95064, USA

<sup>b</sup> Monterey Bay Aquarium Research Institute, 7700 Sandholdt Road , Moss Landing, CA 95039, USA

## Abstract

The effects of the 1997–1999 El Niño/La Nina event on new primary production are examined using a physiologically based algorithm of nitrate uptake by phytoplankton for the Monterey Bay, California region. Primary inputs for the model come from temperature and phytoplankton biomass (chlorophyll) using both moorings and satellite observations, providing estimates of new production with higher spatial and temporal resolution as compared to traditional shipboard measurements. We observed significant decrease in new production values during the El Niño event, and a corresponding enhancement during La Niña as compared to the values during the El Niño period. The observed interannual changes in new production varied as a function of distance from shore, consistent with the hypothesis that productivity offshore from the upwelling center was impacted because of the suppression of the thermocline and nitracline associated with the ENSO event. There was less evidence for a significant downstream trend in new production values, suggesting that distance from shore is the predominant variable in spatial estimates of new production. © 2002 Elsevier Science Ltd. All rights reserved.

## Contents

1. Introduction . . . . .	234
2. Model description and validation . . . . .	235
2.1. Moorings . . . . .	236
2.2. Satellite . . . . .	238
2.3. Temperature . . . . .	238
2.4. Kinetic parameters . . . . .	240
2.5. New production . . . . .	241
2.6. Product validation . . . . .	241

\* Corresponding author. Tel.: +1-831-459-3290; fax: +1-831-459-4882.  
E-mail address: kudela@cats.ucsc.edu (R.M. Kudela).

3. Results and discussion . . . . .	243
-------------------------------------	-----

---

## 1. Introduction

The introduction of the Sea-Viewing Wide Field-of-View Sensor (SeaWiFS) ocean color instrument in the autumn of 1997 occurred shortly after the onset of perhaps the largest El Niño event of the century, providing us with the opportunity to monitor the impact of such events on biological and bio-optical properties in central California. During a typical (non-El Niño) year, the Monterey Bay region can be characterized by three oceanographic periods, corresponding to a spring/summer ‘upwelling season’, a summer/fall ‘oceanic season’, and a winter ‘Davidson season’ (Skogsberg, 1936; Skogsberg & Phelps, 1946). The onset of the 1997–1998 El Niño event was observed in Monterey Bay primarily as a ‘dampening’ of the normally strong but sporadic spring upwelling conditions, which are characterized by the presence of a cold (10–11 °C), salty (33.4–33.8) plume of upwelled waters with associated elevated phytoplankton biomass (chlorophyll) and primary production (Pennington & Chavez, 2000). Although 1997 began with springtime conditions similar to climatological patterns (Pennington & Chavez, 2000), the onset of El Niño conditions caused a substantial warming of the surface waters, with a corresponding decrease in nutrient availability and phytoplankton growth. Here, we examine the impact of this El Niño event on biological production by using a combination of satellite and mooring data to model the changes in new primary production using a simple algorithm-based approach, with particular emphasis on the spatial redistribution of phytoplankton biomass and production.

Monterey Bay, California is located on the eastern edge of the California Current system, and is a classic example of an eastern boundary current regime. In any given year, Monterey Bay will experience several pulses of strong upwelling-favorable winds that last for several days during the upwelling season (March–September), and are followed by periods of lighter winds or even wind reversals (Breaker & Broenkow, 1994; Rosenfeld, Schwing, Garfield, & Tracy, 1994). During weak upwelling there is typically a persistent source of upwelled waters to the north of Monterey Bay near Davenport, California, whereas several days of upwelling-favorable (northwesterly) winds produce a series of cold, salty plumes along the coast. The spatial and temporal extent of these upwelling plumes is highly variable, and warm, nutrient-depleted waters can still occur in this region during the upwelling season (Pennington & Chavez, 2000).

Associated with these upwelled waters are increased concentrations of macro- and micronutrients in the surface waters, which feed a high-biomass, high-productivity diatom-dominated system from about March–October (Wilkerson et al., 2000). During the rest of the year (oceanic and Davidson periods), surface waters are generally warmer, less salty, and with substantially lower nutrient concentrations. During this period, the phytoplankton assemblage is dominated by a low-biomass picoplankton community (Pennington & Chavez, 2000; Skogsberg, 1936). Much of the diatom-driven productivity during the upwelling season is exported both offshore and downstream from the upwelling centers (Pilskaln, Paduan, Chavez, Anderson, & Berelson, 1996). During El Niño events, conditions are less favorable for upwelling so anomalously warm (nutrient depleted) waters are upwelled and advected towards shore, so reducing the seasonal increase in productivity and subsequent export of organic material (Chavez, 1996; Kudela & Chavez, 2000).

We have previously described the use of a physiologically based model or algorithm of new production (*sensu* Dugdale & Goering, 1967) for the Monterey Bay region (Kudela & Chavez, 2000). The calculations were based on the use of high-frequency temporal data from moorings operated by the Monterey Bay Aquarium Research Institute (MBARI) and the National Data Buoy Center (NDBC), made available by MBARI and the Coastal Studies Program, Scripps Institution of Oceanography, respectively (Fig. 1). With the launch of SeaWiFS ocean color satellite and the continued availability of the Advanced Very High Resolution Radiometer (AVHRR) we can apply this approach to a much larger spatial region, by utilizing the biomass (Chlorophyll; from SeaWiFS) and sea surface temperature (SST; from AVHRR) data fields

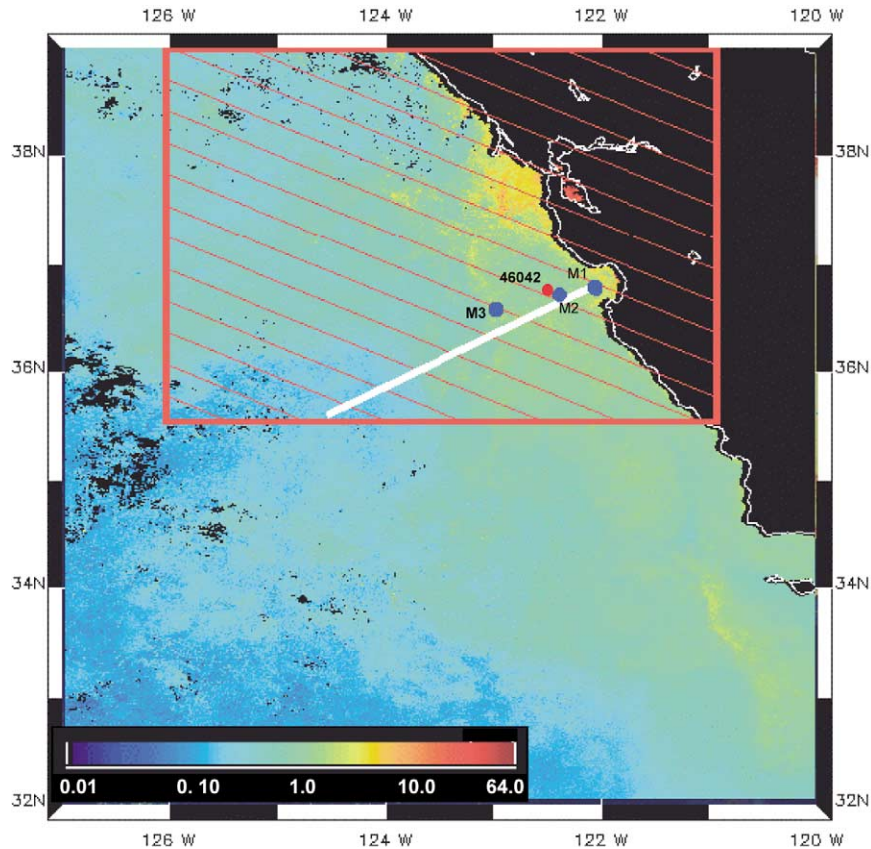


Fig. 1. Map of central California showing chlorophyll concentrations from SeaWiFS (composite image of May, 1998). The Red hatched box indicates the model domain, which was determined by the availability of 1 km resolution AVHRR data from the NOAA Coastwatch program. The white line denotes CalCOFI Line 67. The solid blue circles represent the locations of MBARI moorings M1, M2 and M3, and the red circle represents the location of the NDBC 26042 buoy. The color bar provides chlorophyll concentrations ( $\text{mg m}^{-3}$ ) for the background image.

from these satellites. The main goals of this paper are to demonstrate the applicability of this algorithm to satellite data and to examine the spatial variability of new primary production during this El Niño event. We will demonstrate that there is a significant impact on new production, as was shown for the 1992–1993 event, and we will examine these impacts along an offshore gradient. The general effects (both physical and biological) of ENSO events on coastal California have been well described by others (Bograd & Lynn, 2001; Chavez, 1996; Hayward, 2000; Johnson, Chavez, & Friederich, 1999; Kahru & Mitchell, 1999, 2000; Lenarz, Ven Tresca, Graham, Schwing, & Chavez, 1995; Lynn et al., 1998; Pilskaln et al., 1996; Ramp, McClean, Collins, Semtner, & Hays, 1997) and so will not be discussed in detail here.

## 2. Model description and validation

*Background.* This is an algorithm-based model and was originally developed for use with satellite remote sensing data (Kudela, 1995; Kudela & Dugdale, 1996). It is derived from a model initially described by Dugdale, Davis, and Wilkerson (1997) and Dugdale, Morel, Bricaud, and Wilkerson (1989), and estimates

new production (as  $\text{NO}_3^-$  uptake) based on changes in the physiological status of the phytoplankton assemblage, and corresponding changes in nitrogen utilization (Kudela, Cochlan, & Dugdale, 1997; Kudela & Dugdale, 2000). This approach is similar in structure to the more widely used primary productivity algorithms (Behrenfeld & Falkowski, 1997). Briefly, this model includes time- and nutrient-dependent variability in the physiological parameters (acceleration, specific uptake rates) and expands the applicability of the model to include non-upwelling periods, providing the opportunity to estimate an entire seasonal cycle rather than restrict the observations to upwelling events. As a result, the new production estimates are not constrained to predictions of basin-scale regions where box-model calculations can be performed (Carr, Lewis, Kelley, & Jones, 1995; Morin, Wafar, & LeCorre, 1993; Peña, Lewis, & Cullen, 1994). The assumptions and parameters of this model are described in detail elsewhere (Kudela, 1995; Kudela & Chavez, 2000; Kudela & Dugdale, 2000) and the reader is directed to those sources for further details. Here we will provide an overview of the algorithm assumptions and inputs, and describe modifications to the model.

Two iterations are presented; we have run the algorithm using mooring data (as described in Kudela & Chavez, 2000) and using the satellite-derived biomass and SST fields. Neither version of the model resolves vertical structure, and we do not use vertical temperature, pigment, and nutrient data, nor do we include the contribution of light and temperature adaptation by the algal assemblage. Previous work (Olivieri, 1996; Olivieri & Chavez, 2000) has demonstrated that the mixed layer generally accounts for more than half of the integrated primary productivity (and presumably new production) at the M1 mooring site in Monterey Bay. To the extent that the mixed layer is homogenous and M1 is representative of the study region, our estimates will represent ca. >50% of the depth integrated new production as well. Since depth-integrated new production is more ecologically relevant than mixed-layer values, we also provide a comparison of our estimates to depth-integrated bottle measurements using the stable isotope  $^{15}\text{N}$ , as an indicator of surface new production estimates for determining depth-integrated values. Again, we are not explicitly modeling depth-integrated production, but this comparison provides a basis for evaluating the utility of mixed-layer new production estimates. The mooring data represent a single depth (surface new production values), while the satellite data represent a mean new production value over the first optical depth, which is typically shallower than the mixed layer depth in Monterey Bay. As such, both the mooring and satellite versions of the model presented here can be considered first approximations of the mixed layer new production values.

As inputs to this model we provide biomass (as chlorophyll), SST, day length (calculated from the year-day and latitude), and an estimate of the temperature of the source, or upwelling, water (see Table 1 for parameters). From these inputs several data fields are determined as described by Kudela and Chavez (2000). The calculations are essentially the same for the mooring and satellite versions of the model. Previous use of this model (Kudela & Chavez, 2000) demonstrated that the impact on estimates of new production during the 1992–1993 El Niño was most apparent (defined as the greatest difference from the climatological conditions) from year-days (YD) 90–180, or the upwelling season, presumably as a result of the anomalously warm surface waters and low biomass during that period. Inclusion of the other time periods (YD 0–90, 180–365, or the Davidson and oceanic periods) significantly reduced the apparent impact of the 1992 event on new production; for this reason, we have focused on the period YD 90–180 for this analysis using the satellite data, where we expect to see the greatest impact of the 1997–1998 event. We also provide daily and annual estimates of new production at the mooring locations (Table 2, Fig. 3).

### 2.1. Moorings

Data were provided from four mooring locations (Fig. 1). The Monterey Bay Aquarium Research Institute (MBARI) maintains a series of moorings equipped with temperature sensors and fluorometers at multiple depths (Chavez et al., 1997). For this study, data from the M1, M2, and M3 moorings were utilized. The M3 mooring (furthest offshore) was deployed during the 1997–1998 El Niño event, and so data were only available for 1998 and 1999 at that location. Temperature data from National Data Buoy Center 46042

Table 1  
Input parameters and other symbols used in this model

Parameter	Value	Description	Source
<i>Model input data</i>			
$D$	$\text{h d}^{-1}$	Daylength (daylight hours)	Kirk, 1994
Chl $a$ (mooring)	$\text{mg m}^{-3}$	Fluorescence-based biomass	MBARI mooring fluorometers
Chl $a$ (SeaWiFS)	$\text{mg m}^{-3}$	OC2v2 algorithm biomass	SeaWiFS HRPT satellite data
$T$ (mooring)	$^{\circ}\text{C}$	SST	MBARI moorings
$T$ (AVHRR)	$^{\circ}\text{C}$	NOAA-NESDIS MCSST	NOAA-14 night-time satellite data
<i>Temperature-nitrate relationship</i>			
Climatological nitrate	$0.510T^2 - 16.64T + 134.5$	$T:N$ regression	MBARI time series, 1989–1999
1997 Nitrate	$0.366T^2 - 12.87T + 112.5$	$T:N$ regression	MBARI time series, 1997
1998 Nitrate	$0.332T^2 - 12.16T + 107.1$	$T:N$ regression	MBARI time series, 1998
1999 Nitrate	$0.384T^2 - 14.00T + 119.7$	$T:N$ regression	MBARI time series, 1999
<i>Temperature-age relationship</i>			
$\Delta T$	$0.5^{\circ}\text{C d}^{-1}$	Heating rate	Drifter studies, 1989–1995
$T_{60}$	$^{\circ}\text{C}$	Temperature at 60 m	MBARI moorings, 1989–1995
<i>Kinetics parameters</i>			
$V_0$	$7.5 \times 10^{-3} \text{h}^{-1}$	Initial specific uptake rate	Shipboard experiments, 1992–1993
$K_s$	$1.0 \text{mg}^{-1} \text{at N m}^{-3}$ ( $ \text{NO}_3  > 1$ ) $0.1 \text{mg}^{-1} \text{at N m}^{-3}$ ( $ \text{NO}_3  < 1$ )	Half-saturation constant for $\text{NO}_3$ uptake	Shipboard experiments, 1992–1993
$A_{\text{max}}$	$1.34 \times 10^{-3} \text{h}^{-2}$	Max. potential acceleration rate	Shipboard experiments, 1992–1993
$\tau_{A_{\text{max}}}$	64.8 h	Time to $A_{\text{max}}$	Shipboard experiments, 1992–1993
<i>Other relevant symbols</i>			
$T, T_{\text{SST}}, T_{60}$	$^{\circ}\text{C}$	Temperature (subscript denotes specific depth)	
$t_w$	days	Age of the upwelled water	
$A_t$	dimensionless	Shaping function which defines the change in acceleration at time $t$	
$V'_{\text{max}}$	$\text{h}^{-1}$	Maximum specific $\text{NO}_3$ uptake rate (assuming complete shift-up)	
$V_{\text{max}}(t)$	$\text{h}^{-1}$	Maximum specific $\text{NO}_3$ uptake rate at time $t$	
$V_m$	$\text{h}^{-1}$	Modeled specific $\text{NO}_3$ uptake rate	
$\rho$	$\text{mg-at N m}^{-3} \text{d}^{-1}$	New production (volume transport rate)	

Table 2

New production estimates from mooring sites M1, M2, and M3. New production values are given as daily-averaged values (mg-at N m<sup>-3</sup> d<sup>-1</sup>) for the year ( All Days), or the upwelling season (YD 90-180). Climatological values are the average for 1990–1999. Values in parentheses provide 1 SD

	All days		YD 90-180		
	M1	M2	M1	M2	M3
Climatology	0.870 (1.205)	0.361 (0.561)	2.393 (1.460)	1.083 (0.677)	
1997	0.497* (0.712)	0.485* (0.577)	0.636* (0.540)	0.842* (0.694)	
1998	0.437* (0.583)	0.209* (0.723)	0.487* (0.469)	0.181* (1.074)	0.005 (0.016)
1999	0.628* (0.932)	0.468 (0.732)	1.557* (1.127)	1.074 (1.041)	0.445 (0.387)

\*Values significantly different from the climatology using a two-tailed *t*-test with unequal variance ( $P < 0.05$ ).

were used to fill in missing data for M2 as necessary. The fluorometer readings (volts) were converted to chlorophyll estimates using an empirical relationship derived from simultaneous fluorescence and extracted chlorophyll measurements.

## 2.2. Satellite

Data from SeaWiFS were provided by the MBARI High Resolution Picture Transmission (HRPT) ground station, where data are archived at 1 km pixel (nominal) resolution for central California. SeaWiFS imagery was collected at MBARI and processed using the best available ancillary (ozone and meteorological corrections) data by the Goddard Space Flight Center using the OC2v2 algorithm, second reprocessing (O'Reilly et al., 1998). SST data were collected from the NOAA-14 satellite and processed using the NOAA-NESDIS nighttime non-linear multi-channel SST algorithm. The ocean color and temperature data were co-registered using the SeaDAS package (Fu, Baith, & McClain, 1998). Satellite data were binned using an 8-day geometric (chlorophyll) or arithmetic (SST) mean before further processing; the geometric mean is the appropriate calculation for chlorophyll (Campbell, 1995) and would slightly lower the mean SST as compared to an arithmetic mean (but well within 1 standard deviation of the arithmetic mean SST). The study region (Fig. 1) was chosen based on the availability of 1 km SST products from the NOAA Coastwatch program. New production values were calculated using the 8-day averaged data. These results were then binned for the period YD 90-180, which corresponds to the upwelling season for central California. This temporal averaging was done both to increase the data density (within any given 8-day bin, numerous pixels were masked by clouds) and to facilitate comparison of the trends in new production between 1998 and 1999. For the mooring data, daily results were smoothed using a 10-day running mean and binned for the entire year and for the YD 90-180 period (Table 2).

## 2.3. Temperature

Surface nitrate concentrations and the age of the water were estimated using the SST data ( $T$ , °C) from the moorings or satellite. Nitrate concentrations were estimated using a quadratic polynomial function, parameterized with discrete temperature and NO<sub>3</sub> values collected between 1988–1999 in Monterey Bay. All values for temperatures greater than 8.0 °C (the coldest upwelled waters observed in this region) were used for the calculations. Although non-linear models are not significantly better than a simple linear function, the modeled new production values are very sensitive to the zero-nitrate intercept, which by definition results in zero new production. Therefore, the non-linear models were chosen because of the

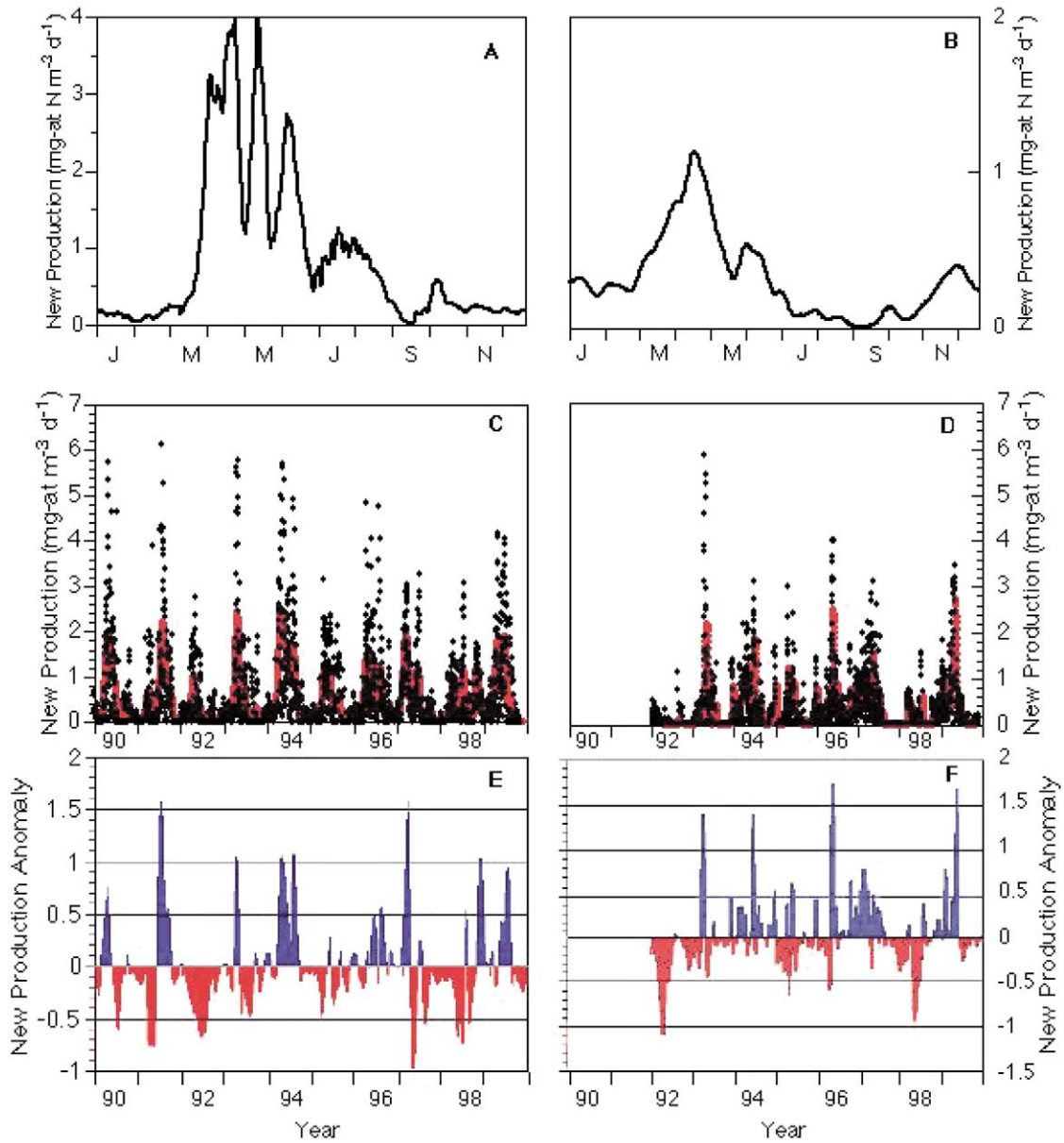


Fig. 3. Modeled new production values from the M1 mooring are plotted for 1990–1999. The top panel provides daily anomalies (daily values minus the climatological mean daily value for 1990–1999) and the lower panel provides daily new production values. The solid red line in the lower plot is a 10 day running mean.

greater latitude in temperatures before zero nitrate values were predicted. Three separate functions were used for 1997, 1998, and 1999, while a composite of all data from 1988–1999 was used for the climatology:

$$[\text{NO}_3] = 0.366T^2 - 12.87T + 112.5; n = 857, r^2 = 0.91(1997) \quad (1a)$$

$$[\text{NO}_3] = 0.332T^2 - 12.16T + 107.1, n = 812, r^2 = 0.91(1998) \quad (1b)$$

$$[\text{NO}_3] = 0.384T^2 - 14.00T + 119.7, n = 112, r^2 = 0.89(1999) \quad (1c)$$

$$[\text{NO}_3] = 0.510T^2 - 16.64T + 134.5, n = 7828, r^2 = 0.89(1988–1999) \quad (1d)$$

Since this model relies on a time-dependent physiological adaptation of the phytoplankton assemblage, it is also necessary to determine the apparent age of the water mass, where age refers to time since upwelling or time since physiological perturbation. To adapt this model to mooring data, a composite-year temperature field at 60 m depth was created, which corresponds to the approximate depth of the upwelled source water at the M1 time-series location (Olivieri, 1996). The age of the water ( $t_w$  days) at each time step is then determined by assuming a constant rate of change in the water temperature, expressed as  $\partial T/\partial t$ :

$$t_w = T_{\text{SST}} - T_{60} / (\partial T/\partial t) \quad (2)$$

where  $\partial T/\partial t = 0.5^\circ\text{C d}^{-1}$ . This value was chosen based on drifter track studies performed in Monterey Bay from 1990–1995, and is comparable to similar eastern boundary current upwelling regimes (Dugdale et al., 1997), including Point Conception, California ( $0.49^\circ\text{C d}^{-1}$ ),  $15^\circ\text{S}$  Peru ( $0.5^\circ\text{C d}^{-1}$ ) and Cap Blanc, northwest Africa ( $0.56^\circ\text{C d}^{-1}$ ). Although parameterized for Monterey Bay, recent studies in northern California corroborate this coefficient (Bruland, personal communication; Kudela, unpublished data). This value is consistent with a daily solar insolation of  $400\text{ W m}^{-2}$  and an average mixed layer depth of 8 m (Olivieri & Chavez, 2000), assuming all of the incoming radiation is converted to heat and ignoring advection and diffusion. We also tested the  $t_w$  parameter using the coldest SST pixel from the satellite data within the study region; there was not a significant difference in new production values between the coldest pixel method and the 60 m temperature as a proxy for upwelled water.

#### 2.4. Kinetic parameters

Several constants related to the physiological activity of the phytoplankton need to be defined for this model. These parameters are described in Kudela and Chavez (2000) and Kudela and Dugdale (2000), and were not modified for this model run. They are as follows, and summarized in Table 1:

$$V_0(\text{h}^{-1}) = 7.5 \times 10^{-3} \quad (3)$$

where  $V_0$  is the initial biomass-specific uptake rate, which defines the lowest non-zero uptake rate for the region (equivalent to a baseline uptake rate).

$$K_s(\text{mg-atNO}_3\text{-N m}^{-3}) = 1.0 \text{ if } [\text{NO}_3] > K1, K_s = 0.1 \text{ if } [\text{NO}_3] < 1 \quad (4)$$

where  $K_s$  the half-saturation constant for  $\text{NO}_3$  uptake; assuming Michaelis–Menten nutrient uptake kinetics for field assemblages of phytoplankton.

$$A_{\text{max}}(\text{h}^{-2}) = 1.34 \times 10^{-3} \text{h}^{-1}(D/24\text{hd}^{-1}) \quad (5)$$

where  $A_{\text{max}}$  is the potential maximum acceleration rate, scaled to a 24 hour day, and assuming no uptake at night. This parameter sets how fast a phytoplankton community can acclimate to optimal growth conditions, and can be thought of as a lag-phase in growth.

$$A_t = \exp -x(t - \tau_{A_{\text{max}}})^2; x = 0.5 \text{ if } t < 2.7; x = 0.08 \text{ if } t > 2.7 \quad (6)$$

$$\tau_{A_{\text{max}}}(\text{h}) = 64.8 \quad (7)$$

where  $A_t$  is the time-dependent function of acceleration (dimensionless), or a weighting factor which changes  $A$  (acceleration) as a function of time.  $\tau_{A_{\text{max}}}$  is the length of time it takes before the maximum acceleration value Eq. (5) is reached. These parameters set the lag phase in growth (or new production), and the ‘shape’ of the resulting increase and decrease in new production as a function of time.

### 2.5. New production

The model predicts specific  $\text{NO}_3^-$  uptake rates ( $V$ ,  $\text{h}^{-1}$ ) and must be normalized to biomass for an estimate of volume transport rates or new production ( $\rho$   $\text{mg-at N m}^{-3} \text{ h}^{-1}$ ) and converted to per day units for ease of interpretation. Since particulate nitrogen (PN) values (necessary to convert  $V$  values to  $\rho$  values) are not available from remotely sensed data, we estimated PN from a polynomial-fit composite-year of chlorophyll values (Kudela & Chavez, 2000). PN was estimated from chlorophyll using the relationship  $1 \text{ mg-at N m}^{-3} = 1 \text{ mg Chl m}^{-3}$  (Eppley, Chavez, & Barber, 1992). This value is consistent with the bottle data used for model validation ( $1.14 \pm 0.52$ ,  $n = 92$ ; mean  $\pm$  SD), and with published values for Monterey Bay ( $1.32 \pm 0.51$ ,  $n = 17$ , Kudela & Dugdale, 2000;  $0.98$ ,  $n = 38$ , Wilkerson et al., 2000). Because we use a PN:Chl conversion factor, these estimates may also be considered similar to measurements of  $V^{\text{chl}}$  as described by Dickson and Wheeler (1995), which has been suggested as being a more appropriate measure of new production, since it is not influenced by detrital PN.

New production was determined as:

$$\rho(\text{mg-at N m}^{-3} \text{ d}^{-1}) = V_m \text{Chl}[\text{mg-at N m}^{-3}] / (\text{mg Chl m}^{-3}) D \quad (8)$$

where  $D$  is the daylength determined for the latitude of each pixel or mooring location. This model assumes no dark uptake of  $\text{NO}_3^-$  at night, and constant uptake during daylight hours (based on previous experiments; Kudela, 1995).

### 2.6. Product validation

This model has previously been compared to direct shipboard measurements of new production using the stable isotopic tracer  $^{15}\text{N}$  from 100 and 50% light penetration depth (LPD; Kudela & Chavez, 2000). For this time period (1997–1999), we have 10 additional  $^{15}\text{N}$  data points from 1997–1998, increasing the total validation set to 46 discrete stations, or 92 data points from 100 and 50% LPD, collected between 1989–1998, predominantly near the M1 mooring site. We have also used the full depth profiles from the 46 stations to calculate a depth-integrated new production value, which is more ecologically relevant than using surface values only. Using these data, we recalculated the regression between observed and predicted data using the surface values and the depth-integrated values to see how well the estimated (mooring or satellite) values compared to comparable (surface) or depth-integrated estimates. The results were essentially the same as reported previously, with an  $r^2$  value of 0.74 for the near-surface values and 0.72 for the depth-integrated values. We also determined the mean square prediction error (MSPE), which does not assume linearity between the observed and predicted values, and provides an error estimate with the same units as the modeled data for variance and standard deviation values (Neter, Wasserman, & Kutner, 1990). The algorithm-based method predicts new production within  $\pm 0.80 \text{ mg-at N m}^{-3} \text{ d}^{-1}$  ( $\pm 1\text{SD}$ ) for all (depth integrated) data.

Previous sensitivity analyses of this model (using satellite data for inputs) provide boundaries for the error introduced from model parameterization (Kudela, 1995). Values for  $K_s$ ,  $V_i$ ,  $A_{\text{max}}$ ,  $\tau_{A \text{ max}}$  and  $\partial T / \partial t$  were manipulated by  $\pm 50\%$  of the defined values, while the  $T:\text{NO}_3$  regression was manipulated by  $\pm 1$  SD for the slope and intercept values using a linear equation. For the estimates presented here, we have not used a linear  $T:\text{NO}_3$  function. However, except at low  $\text{NO}_3$  values, the linear and polynomial functions provide statistically similar values, and model sensitivity to the linear function is assumed to be a reasonable indicator of performance with the polynomial function. Resulting model output (as  $V_m$ ,  $\text{h}^{-1}$ ) was relatively insensitive to most of these manipulations, with  $V_m$  fluctuating between  $\pm 4$ – $19\%$ , which is within the coefficient of variation for bottle incubations using  $^{15}\text{N}$ . Estimates of new production were similarly affected by changes in the model parameters, although the uncertainty in the PN:Chl term adds another source of variance to the new production values. Since the estimated new production ( $\text{mg-at N m}^{-3} \text{ d}^{-1}$ ) is a direct

function of the PN:Chl ratio, any changes in this ratio would cause a corresponding change in the estimated new production values.

With the addition of the SeaWiFS chlorophyll data, we have obviously introduced another source of error into our estimates since we are using satellite-derived pigments to determine PN. To verify whether the SeaWiFS data significantly bias biomass estimates, we tested the OC2v2 chlorophyll algorithm with a regional dataset of bio-optical and chlorophyll measurements. There are known biases in the OC2v2 algorithm for central California compared to other oceanic provinces, with a slight underestimate at moderate ( $1\text{--}10\text{ mg m}^{-3}$ ) chlorophyll levels and overestimates at the extremes ( $0.1\text{--}1.0$  and  $>10\text{ mg m}^{-3}$  Chl, Fig. 2; see also Kahru & Mitchell, 1999). The errors associated with the OC2v2 algorithm were of the same range as for the database used to parameterize the SeaWiFS global processing algorithms (O'Reilly et al., 1998). We also tested this regional database against several other published algorithms including the OC4v4 and CAL-P6 algorithms (Kahru & Mitchell, 1999; O'Reilly et al., 1998). All of these algorithms performed similarly in terms of RMS error, and we do not expect significant differences in estimated new production resulting from reprocessing the SeaWiFS data using alternate algorithms.

To compare the performance of our predicted new production values using mooring versus satellite data,

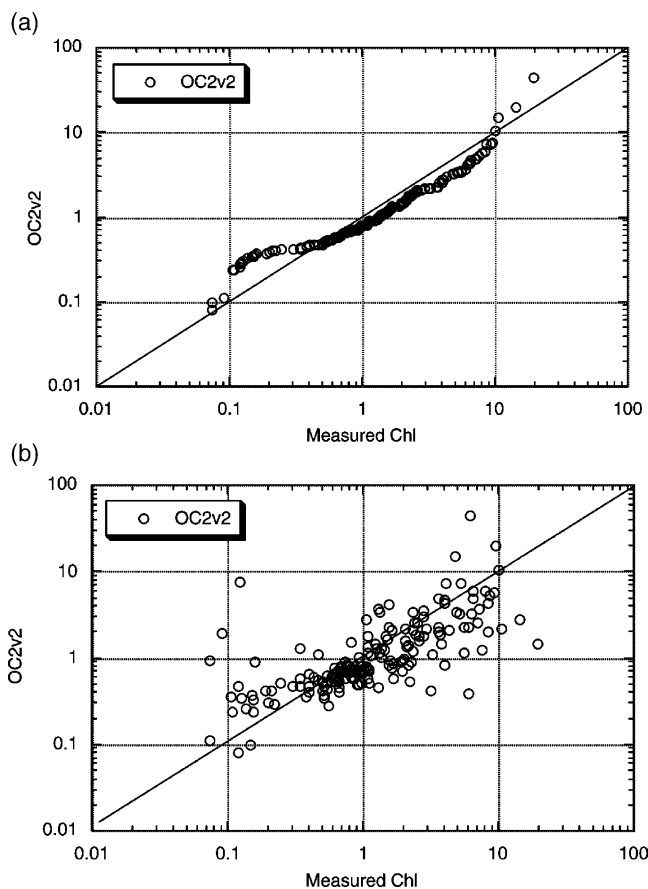


Fig. 2. Modeled versus measured chlorophyll *a* values from the MBARI bio-optical database (in situ measurements) using the OC2v2 chlorophyll algorithm. The top panel represents the quantile–quantile plot of the data, while the bottom panel provides a scatter plot of the same data. Statistical parameters for these data are: slope, 1.212; intercept,  $-0.053$ ; RMS error, 0.351; MSPE,  $0.123\text{ mg Chl m}^{-3}$ . The MSPE value represents the error in chlorophyll units.

we estimated new production using satellite SST and chlorophyll values for the M1, M2, and M3 moorings during 1999. There were a total of 68 days when we had co-located SST and chlorophyll data at the three mooring locations together with good mooring fluorometer and temperature data. New production values were determined independently at each site using either satellite or mooring inputs, and compared using the instantaneous (satellite) and day-averaged (mooring) data. The mooring versus satellite results provide new production estimates within  $1.27 \text{ mg-at N m}^{-3} \text{ d}^{-1}$  (MSPE). This is less robust than the mooring versus bottle comparisons ( $0.80 \text{ mg-at N m}^{-3} \text{ d}^{-1}$ ), which can be attributed to, first the differing spatial and temporal integration, and secondly the variability in the satellite versus mooring SST and chlorophyll. For the same 68 data points, the MSPE for SST was  $1.78 \text{ }^{\circ}\text{C}$  (RMSerror = 12.27%), and the MSPE for Chlorophyll was  $6.89 \text{ } \mu\text{g Chl}$  (RMSerror = 104.9%). There was no significant positive or negative bias in the comparison, and we conclude that the satellite estimates are reasonably robust as compared to the mooring predictions and  $^{15}\text{N}$  bottle data. All of the predicted results (mooring or satellite) produce errors that are within the errors associated with  $^{15}\text{N}$  measurements (MSPE =  $0.20\text{--}1.40 \text{ mg-at N m}^{-3} \text{ d}^{-1}$ ; Kudela & Chavez, 2000).

This model is parameterized with data from several years of shipboard and laboratory experiments conducted predominantly with Monterey Bay and CalCOFI Line 67 stations. Therefore, the applicability of this model is greatest in this region; although we have extended the model results to include a much larger (remote sensing) domain, these predictions are dependent upon the general applicability of the model parameterizations to central California. Recent work in northern California (Kudela, unpublished) suggests that this is a reasonable assumption; however, we have limited the interpretation of these model results primarily to the general region of CalCOFI Line 67.

### 3. Results and discussion

Chavez (1996) demonstrated that there was a significant ENSO signal in Monterey Bay during 1992, characterized by abnormally warm temperatures and low surface nitrate concentrations, but with a negligible decrease in seasonal primary production and biomass, both in terms of chlorophyll concentrations and in the species composition at the M1 mooring site. During the 1997–1998 event, standing stocks of chlorophyll were again within the climatological mean for 1984–1998 in California (Lynn et al., 1998). As with the 1992–1993 event, there was a much more pronounced effect on chemical and physical properties, with mean annual nitrate concentrations during 1998 decreasing from a climatological value of  $6.2 \text{ } \mu\text{g-at m}^{-3} \text{ NO}_3$  to  $3.3 \text{ } \mu\text{g-at m}^{-3} \text{ NO}_3$ , while SST increased from  $12.7$  to  $13.8 \text{ }^{\circ}\text{C}$ .

The physical conditions associated with El Niño events (a depressed nutricline, warmer temperatures) result in a reduction of the spatial extent of high (new) productivity waters fed by eastern boundary current upwelling plumes (Barber & Kogelschatz, 1990). Chavez (1996) predicted that this biological insensitivity to the 1992 ENSO event was because of the proximity of the phytoplankton productivity stations to the upwelling center near shore. Given the station proximity to the upwelling center, the phytoplankton assemblage was hypothesized to maintain high productivity rates and biomass by stripping the available nutrients from the water column as it moved offshore and downstream from the upwelling center. The M1 mooring site is located in the center of a bifurcated upwelling plume that develops off Davenport, California. This plume produces both an equatorward and offshore filament (Rosenfeld et al., 1994), and the M1 site is exposed to cold, nutrient rich water even during moderate upwelling events because it is located close to and downstream from this upwelling source. Kudela and Chavez (2000) predicted that during El Niño events, levels of new production at the M1 site would be maintained more closely to the climatological mean than at other sites located either further offshore or downstream from the upwelling center, but could not test their hypothesis with the then existing data set. This reduction further downstream or offshore from M1 was hypothesized to occur because the phytoplankton would remove a greater proportion of the

available nitrate from the surface waters to maintain the high biomass and productivity levels observed at M1, leaving less nitrate for assemblages further downstream from the upwelling center. With the application of satellite data sets, we are now in a position to quantify this phenomenon at locations other than mooring sites in Monterey Bay.

During the period 1997–1999, we ran the model using data from the M1, M2 and M3 moorings located inshore to offshore, respectively (Fig. 1). Although we have insufficient data to provide a climatological mean value for new production at the M3 mooring location, we can predict values for 1998 and 1999. During 1997, upwelling-favorable conditions were initiated early in the year, with very strong upwelling and biological production occurring in March (Johnson, Chavez, & Friederich, 1999), prior to the onset of El Niño conditions around July, 1997 (Lynn et al., 1998). El Niño conditions were prevalent through the summer and fall of 1998, whereas 1999 exhibited La Niña physical oceanographic conditions (Hayward et al., 1999).

The model results from the M1, M2, and M3 moorings corroborate the timing of this general picture. During 1997, there was an initial pulse of new primary production at M1 (Fig. 3), which was followed by a prolonged period of generally lower production values until spring 1999. Note, however, that at M1, the mean annual new production and maximal new production values were similar for the 1992–1993 and 1997–1998 El Niño periods and for non-El Niño years, in particular 1995 (Fig. 3). Seasonally integrated values of modeled new production values from M1 generally demonstrate lower new production values (30–50%) for 1997–1999 relative to the mean climatology (Table 2), although this reduction is not statistically significant. Within the three-year study period, 1998 (the peak of the El Niño period) exhibited lower mean values than either 1997, when there was an early and strong upwelling season prior to the onset of El Niño conditions, or 1999, during which central California recovered. Further offshore, the range in production at the M2 mooring was more extreme compared to the mean climatology; there was with a 33% enhancement during 1997, a 42% decline in 1998, and 31% enhancement in 1999 (Table 2). As reported previously (Kudela & Chavez, 2000), the bulk of the seasonal new production in the model domain occurs from YD 90–180. Using this time window, the changes in new production are more readily apparent. There was a significant decline in new production values at the inshore moorings during both 1997 and 1998 (the El Niño period), and a return to climatological conditions during 1999 (Table 2).

For comparison to the 1997–1998 event, we can consider the impact of the 1992–1993 El Niño on new production in Monterey Bay at M1 and M2, which has previously been described using a version of this algorithm (Kudela & Chavez, 2000). It is not possible to compare the previously published values directly, since we have modified the model (e.g. the change in regression equations for the temperature:nitrate conversion) and use differing climatological values (1990–1996 versus 1990–1999). For the most recent climatology, these data (including 1997–1999) increased the annual new production from 287 to 318 mg-at N m<sup>-3</sup> y<sup>-1</sup>, and from 187 to 132 mg-at N m<sup>-3</sup> for the period YD 90–180. At the M2 site, the climatological new production was very nearly the same.

During the 1992–1993 event, the decrease in new production was most apparent during the ‘upwelling season’ from YD 90–180, 1992, with a 70% (M1) and 96% (M2) decrease compared to the climatology. In contrast, the annual new production values declined 71% (M1) and 61% (M2). In this more recent event, new production was reduced at the M1 mooring during both 1997 and 1998 as compared to the climatology (50% reduction in both years), with an even greater impact during the YD 90–180 period (80, 73% reductions for 1997 and 1998). In contrast, the M2 mooring location demonstrated an annual increase of 34% in 1997 and a 42% decrease in 1998, with a net decrease of 22 and 83% during YD 90–180 (1997 and 1998, respectively). These findings are consistent with the 1997–1998 event being the ‘El Niño of the century’, with a significantly greater temporal impact than the 1992 event. Spatially, 1998 exhibited a uniform decrease at M1 and M2 (50% reductions), and a gradient in impact from onshore (M1) to offshore (M2) during 1997. We attribute the increase in new production (34%) at M2 during 1997 to the early onset of strong upwelling conditions, which preceded the El Niño event (Johnson et al., 1999). This event

was both unseasonably early and spatially extensive in the offshore direction, and clearly affected the mean new production values at M2 as compared to the climatology; during this event, peak estimates of new production at M2 approached the climatological maximal values predicted for M1, located several kilometers closer to the upwelling source.

We do not have sufficient data to produce a climatological mean value for new production at the M3 mooring location. However, we see an almost 100-fold increase in modeled new production values from 1998 to 1999 during the upwelling period (YD 90-180; Table 2). These observations are consistent with the hypothesis that El Niño events result in a collapsing inward of productivity as both the offshore and downstream extent of cold, nutrient rich waters is reduced. Similarly, we would expect a substantial increase in offshore productivity (at M3) during years of abnormally strong coastal upwelling. These mooring results are consistent with the idea that new production at offshore stations is more susceptible to pronounced decreases during El Niño years, and to pronounced increases during La Niña years, as the upwelling-dominated regime either contracts or expands.

Examination of the composite satellite imagery (YD 90-180) for chlorophyll and temperature provides a similar spatial result (Fig. 4). There is a general inshore retreat of chlorophyll contours during 1998 as compared to 1999, and SSTs are significantly warmer throughout the model domain. This resulted in an approximately 100% decrease in modeled new production values for 1998 as compared to 1999. We do have insufficient SeaWiFS data for 1997 to run the model using the satellite observations, so we cannot discern enhancement resulting from the La Niña versus reduction resulting from the El Niño events.

The model results show both a large offshore region of reduced new production (corresponding to the region of reduced chlorophyll), and somewhat surprisingly, an area of enhanced new production within a few kilometers of the shore. The offshore reduction in new production is consistent with our hypothesis of an inshore collapse of productive waters, as upwelled nutrients become less available (Chavez, 1996; Kudela & Chavez, 2000). This is also consistent with the results from the moorings. The nearshore enhancement is more difficult to interpret, but it is likely that these data are being contaminated by anomalously high pigment values associated with contamination of the satellite data by suspended sediments and colored dissolved material (Kahru & Mitchell, 1999; O'Reilly et al., 2000; Siegel, Wang, Maritorena & Robinson, 2000). Nevertheless, it is apparent that the large-scale physical processes associated with the El Niño–La Niña events of 1997–1999 had profound effects on both the magnitude and distribution of new primary production.

In Fig. 5, we have plotted results from the model outputs (temperature, chlorophyll) and predictions (new production) along with the difference between 1998 and 1999 along CalCOFI Line 67. As with the mooring data, it is apparent that nearshore (e.g. at M1), the relative effects of the El Niño are considerably reduced, even though the absolute magnitude of the difference in new production ( $\text{mg-at N m}^{-3} \text{d}^{-1}$ ) is considerably greater. This is consistent with the assertion (Chavez, 1996; Kudela & Chavez, 2000) that nearshore, weak but persistent upwelling fuels productivity even during El Niño periods. Moving further offshore, the absolute magnitudes of the difference in new production are considerably reduced, but the relative difference reaches a maximum. Finally, several hundred kilometers offshore, there is essentially no impact from the El Niño event where conditions are predominantly oceanic (warm, low biomass) during both El Niño and non-El Niño years. These results are also consistent with the data for this same series of stations presented by Johnson, Chavez and Friederich (1999), comparing 1997 pre-El Niño conditions with 1998 El Niño conditions.

Visual examination of Fig. 5 provides no indication, however, of a strong decrease in new production values downstream from the upwelling center. This could be caused by at least two factors. First, the 90-day averaging may have smoothed out any upwelling signal, which would be expected to have a much shorter temporal signal of the order of several days (Service, Rice, & Chavez, 1998). However, there were no obvious decreases in the 8-day bins (data not shown). Secondly, and more likely, is that the onshore–offshore gradient dominates spatially, at least for our new production estimates.

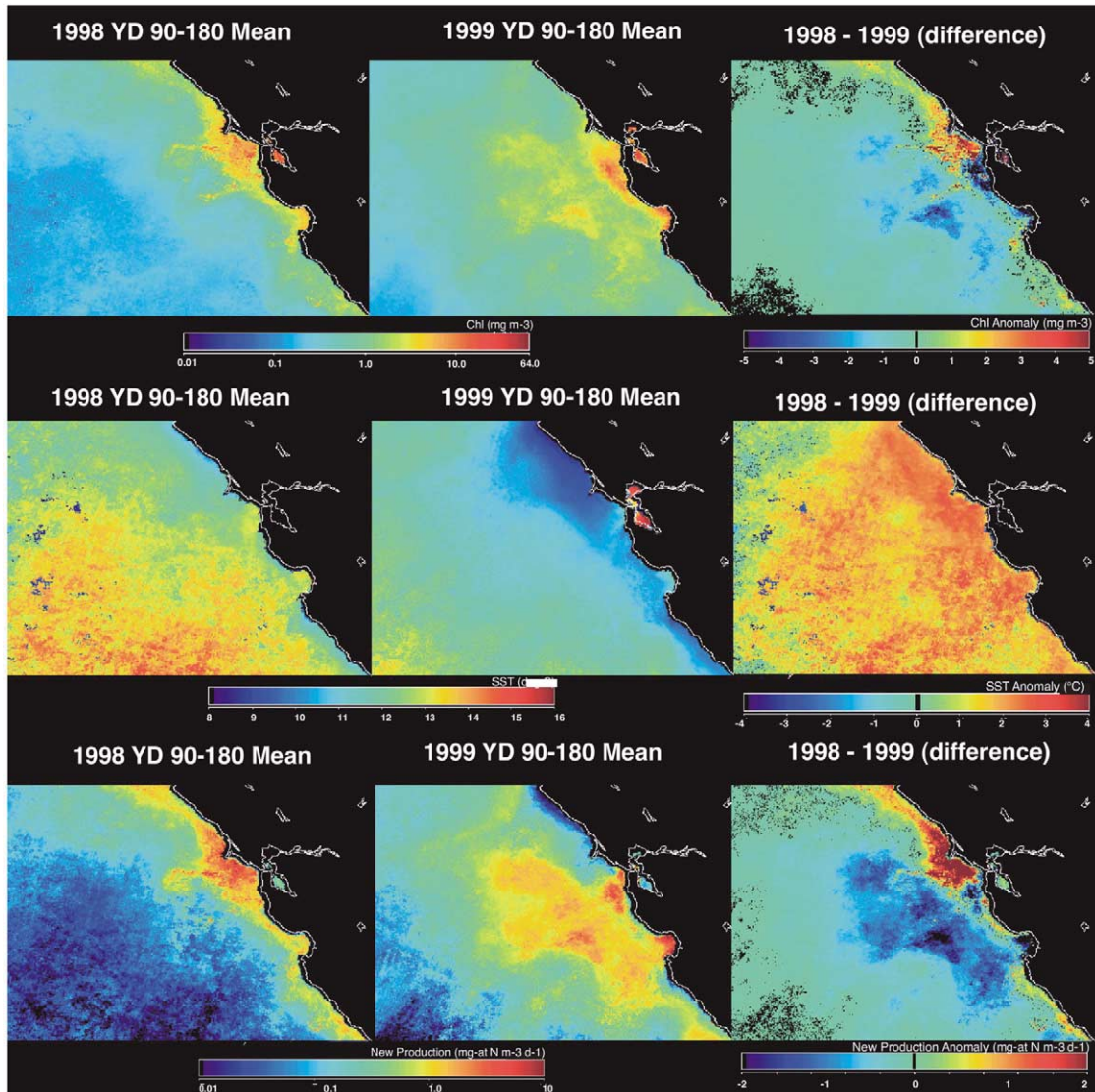


Fig. 4. Composite remote sensing model output for YD 90-180. Top row: Chlorophyll; middle row: SST; bottom row: modeled new production. Within each row, the YD 90-180 composite (mean) provides data for 1998 (left), 1999 (middle), and the difference (1999–1998). Color bars represent chlorophyll ( $\text{mg Chl m}^{-3}$ ), temperature ( $^{\circ}\text{C}$ ), and new production ( $\text{mg-at N m}^{-3} \text{d}^{-1}$ ).

To summarize, a model of new production is presented which utilizes mooring or satellite data (chlorophyll, SST) as primary inputs. During the 1997–1999 event, new production rates decreased significantly in the near-shore environment. As previously hypothesized, new production rates demonstrated a significantly greater decrease further away from the upwelled, high nutrient plume during the peak upwelling season, as determined from comparison of both the moorings (onshore versus offshore) and satellite data. These impacts are greatest during the upwelling period from YD 90-180, and demonstrate strong onshore–offshore horizontal gradients. There was, however, no compelling evidence from the satellite data

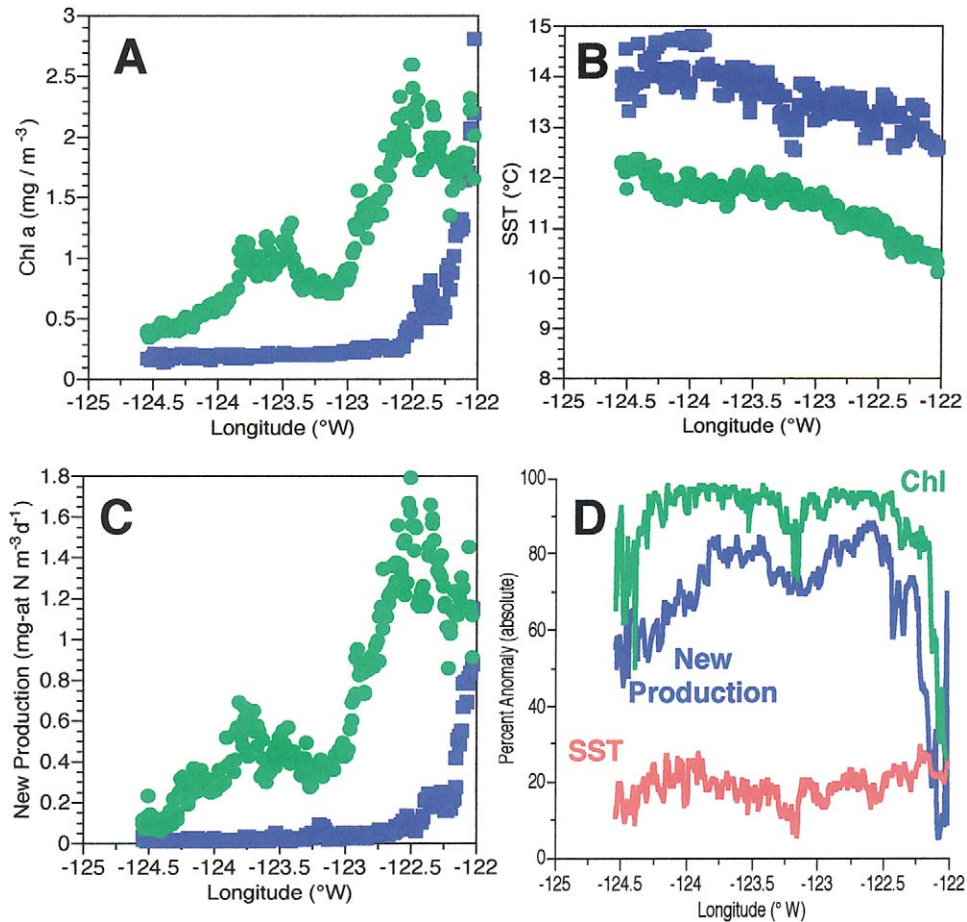


Fig. 5. Chlorophyll (A), SST (B), New Production (C), and the percent difference between 1998 and 1999 (D) from CalCOFI Line 67 are presented for the time period YD 90–180. In Panels A–C, the blue squares represent 1998, the green circles represent 1999. Data points represent approximately 1 km pixels from Fig. 4. In Panel D, The absolute difference is plotted as a percentage. Note that the greatest anomalies occur between ca. 122.5 and 124°W, while the anomalies are reduced close to shore and further offshore. For Panel D, the percent difference was calculated as  $(1998-1999)/1999 \times 100$ .

that there was corresponding down-axis (down the upwelling plume) decrease in new production as previously hypothesized.

### Acknowledgements

R. Michisaki and J. T. Pennington have provided much of the collection and management efforts for the mooring and time series programs, and numerous contributions were also made by MBARI colleagues, as well as the support provided by the crews of the *Point Lobos*, *Point Sur*, and *Western Flyer*. We wish to recognize the support of the David and Lucile Packard Foundation and the National Aeronautics and Space Administration under grants NAG5-8750 and NAG5-8855.

## References

- Barber, R. T., & Kogelschatz, J. E. (1990). Nutrients and productivity during the 1982/83 El Niño. In P. W. Glynn (Ed.), *Global ecological consequences of the 1982–83 El Niño-southern oscillation* (pp. 21–53). New York: Elsevier.
- Behrenfeld, M., & Falkowski, P. J. (1997). Photosynthetic rates derived from satellite-based chlorophyll concentrations. *Limnology and Oceanography*, *19*, 1–12.
- Bograd, S. J., & Lynn, R. J. (2001). Physical–biological coupling in the California Current during the 1997–99 El Niño–La Niña cycle. *Geophysical Research Letters*, *28*, 275–278.
- Breaker, L. C., & Broenkow, W. W. (1994). The circulation of Monterey Bay and related processes. *Oceanography and Marine Biology, An Annual Review*, *32*, 1–64.
- Campbell, J. W. (1995). The Lognormal Distribution as a model for bio-optical variability in the sea. *Journal of Geophysical Research—Oceans*, *100*, 13237–13254.
- Carr, M. E., Lewis, M. R., Kelley, D., & Jones, B. (1995). A physical estimate of new production in the equatorial Pacific along 150°W. *Limnology and Oceanography*, *40*, 138–147.
- Chavez, F. P. (1996). Forcing and biological impact of onset of the 1992 El Niño in central California. *Geophysical Research Letters*, *23*, 265–268.
- Chavez, F. P., Pennington, J. T., Herlein, R., Jannasch, H., Thurmond, G., & Friederich, G. (1997). Moorings and drifters for real-time interdisciplinary oceanography. *Journal of Atmospheric Oceanic Technology*, *14*, 1119–1211.
- Dickson, M. L., & Wheeler, P. A. (1995). Nitrate uptake rates in a coastal upwelling regime—a comparison of PN-specific, absolute and Chl a-specific rates. *Limnology and Oceanography*, *40*, 533–543.
- Dugdale, R. C., Davis, C. O., & Wilkerson, F. P. (1997). Assessment of new production at the upwelling center at Point Conception, California, using nitrate estimated from remotely sensed sea surface temperature. *Journal of Geophysical Research*, *102*, 8573–8586.
- Dugdale, R. C., & Goering, J. J. (1967). Uptake of new and regenerated forms of nitrogen in primary productivity. *Limnology and Oceanography*, *12*, 196–206.
- Dugdale, R. C., Morel, A., Bricaud, A., & Wilkerson, F. P. (1989). Modeling new production in upwelling centers: a case study of modeling new production from remotely sensed temperature and color. *Journal of Geophysical Research*, *94*(C12), 18119–18132.
- Eppley, R. W., Chavez, F. P., & Barber, R. T. (1992). Standing stocks of particulate carbon and nitrogen in the Equatorial Pacific. *Journal of Geophysical Research*, *97*, 655–661.
- Fu, G., Baith, K. S., & McClain, C. R. (1998). SeaDAS: the SeaWiFS data analysis system. In *Proceedings of the fourth Pacific ocean remote sensing conference, Qingdao, China, July 28–31* (pp. 73–79).
- Hayward, T. L. (2000). El Niño 1997–98 in the coastal waters of Southern California: a timeline of events. *California Cooperative Oceanic Fisheries Investigations Reports*, *41*, 98–116.
- Hayward, T. L., Baumgartner, T. R., Checkley, D. M., Durazo, R., Gaxiola-Castro, G., Hyrenbach, K. D., Mantyla, A. W., Mullin, M. M., Murphree, T., Schwing, F. B., Smith, P. E., & Tegner, M. J. (1999). The state of the California Current in 1998–1999: transition to cool-water conditions. *California Cooperative Oceanic Fisheries Investigations Reports*, *40*, 29–62.
- Johnson, K. S., Chavez, F. P., & Friederich, G. E. (1999). Continental-shelf sediment as a primary source of iron for coastal phytoplankton. *Nature, London*, *398*, 697–700.
- Kahru, M., & Mitchell, B. G. (1999). Empirical chlorophyll algorithm and preliminary SeaWiFS validation for the California Current. *International Journal of Remote Sensing*, *20*, 3423–3429.
- Kahru, M., & Mitchell, B. G. (2000). Influence of the 1997–98 El Niño on the surface chlorophyll in the California Current. *Geophysical Research Letters*, *27*, 2937–2940.
- Kirk, J. T. O. (1994). In *Light and photosynthesis in aquatic systems* (2nd ed.) (p. 509). Cambridge: Cambridge University Press.
- Kudela, R. M., 1995. *Characterization and prediction of planktonic nitrogenous nutrition and new production in Monterey Bay, California: nutrient and physiological interactions*. PhD dissertation, University of Southern California, 326 pp.
- Kudela, R. M., & Chavez, F. P. (2000). The impact of the 1992 El Niño on new production in Monterey Bay, California. *Deep-Sea Research II*, *47*, 1055–1076.
- Kudela, R. M., Cochlan, W., & Dugdale, R. C. (1997). Carbon and nitrogen uptake response to light by phytoplankton during an upwelling event. *Journal of Plankton Research*, *19*, 609–630.
- Kudela, R. M., & Dugdale, R. C. (1996). Estimation of new production from remotely-sensed data in a coastal upwelling regime. *Advances in Space Research*, *18*, 91–97.
- Kudela, R. M., & Dugdale, R. C. (2000). Regulation of phytoplankton new production as determined by enclosure experiments with nutrient additions in Monterey Bay, California. *Deep-Sea Research II*, *47*, 1023–1053.
- Lenarz, W. H., Ven Tresca, D. A., Graham, W. M., Schwing, F. B., & Chavez, F. P. (1995). Explorations of El Niños and associated biological population dynamics off central California. *California Cooperative Oceanic Fisheries Investigations Reports*, *36*, 106–119.
- Lynn, R. J., Baumgartner, T., Garcia, J., Collins, C. A., Hayward, T. L., Hyrenbach, K. D., Mantyla, A. W., Murphree, T., Shankle,

- A., Schwing, F. B., Sakuma, K. M., & Tegner, M. J. (1998). The state of the California current, 1997–1998: transition to El Niño conditions. *California Cooperative Oceanic Fisheries Investigations Reports*, 39, 25–49.
- Morin, P., Wafar, M. V. M., & LeCorre, P. (1993). Estimation of nitrate flux in a tidal front from satellite derived temperature data. *Journal of Geophysical Research*, 98(4689-), 4695.
- Neter, J., Wasserman, W., & Kutner, M. H. (1990). In *Applied linear statistical models: Regression analysis of variance and experimental designs* (3rd ed.) (p. 1181). Homewood, IL: Irwin, Inc.
- Olivieri, R. A., 1996. *Plankton dynamics and the fate of primary production in the coastal upwelling ecosystem of Monterey Bay, California*. PhD Dissertation, University of California Santa Cruz, 316 pp.
- Olivieri, R. A., & Chavez, F. P. (2000). A model of plankton dynamics for the coastal upwelling system of Monterey Bay, California. *Deep-Sea Research II*, 47, 1077–1106.
- O'Reilly, J. E., Maritorena, S., Mitchell, B. G., Siegel, D. A., Carder, K. L., Garver, S. A., Kahru, M., & McClain, C. (1998). Ocean color chlorophyll algorithms for SeaWiFS. *Journal of Geophysical Research*, 103, 24937–24953.
- Peña, M. A., Lewis, M. R., & Cullen, J. J. (1994). New production in the warm waters of the tropical Pacific ocean. *Journal of Geophysical Research*, 99(C7), 14255–14268.
- Pennington, J. T., & Chavez, F. P. (2000). Seasonal fluctuations of temperature, salinity, nitrate, chlorophyll and primary production at station H3/M1 over 1989–1996 in Monterey Bay, California. *Deep-Sea Research II*, 47, 947–974.
- Piaskaln, C. H., Paduan, J. B., Chavez, F. P., Anderson, R. Y., & Berelson, W. M. (1996). Carbon export and regeneration in the coastal upwelling system of Monterey Bay, central California. *Journal of Marine Research*, 54, 1149–1178.
- Ramp, S. R., McClean, J. L., Collins, C. A., Semtner, A. J., & Hays, K. A. S. (1997). Observations and modeling of the 1991–1992 El Niño signal off central California. *Journal of Geophysical Research*, 102, 5553–5582.
- Rosenfeld, L. K., Schwing, F. B., Garfield, N., & Tracy, D. E. (1994). Bifurcated flow from an upwelling center: a cold water source for Monterey Bay. *Continental Shelf Research*, 14, 931–964.
- Service, S. K., Rice, J. A., & Chavez, F. P. (1998). Relationship between physical and biological variables during the upwelling period in Monterey Bay, CA. *Deep-Sea Research II*, 45, 1669–1685.
- Siegel, D. A., Wang, M. H., Maritorena, S., & Robinson, W. (2000). Atmospheric correction of satellite ocean color imagery: the black pixel assumption. *Applied Optics*, 39, 3582–3591.
- Skogsberg, T. (1936). Hydrography of Monterey bay, California. Thermal conditions, 1929–1933. *Transactions of the American Philosophical Society*, 29, 1–152.
- Skogsberg, T., & Phelps, A. (1946). Hydrography of Monterey Bay, California, Thermal conditions, Part II, 1934–1937. *Proceedings of the American Philosophical Society*, 90, 350–386.
- Wilkerson, F. P., Dugdale, R. C., Chavez, F. P., & Kudela, R. M. (2000). Biomass and productivity in Monterey Bay, CA: contribution of the larger autotrophs. *Deep Sea Research II*, 47, 1003–1022.